

1 Mechanistic numerical modeling of solute uptake by plant roots  
2 A mechanistic solution for the combined water and solute uptake  
3 by plant roots

4 Andre Herman Freire Bezerra \*      Quirijn de Jong van Lier  
5 Sjoerd E.A.T.M van der Zee

6 January, 2016

\*Bezerra, A.H.F. and Q. de Jong van Lier, Exact Sciences Dep., ESALQ–Univ. of São Paulo, 13418-900 Piracicaba, Brazil; S.E.A.T.M. van der Zee, Dep. of Environmental Sciences, Wageningen Univ., 6708 PB Wageningen, the Netherlands.

## 7 Core ideas

- 8 • idea 1
- 9 • idea 2
- 10 • idea 3
- 11 • optional idea 4
- 12 • optional idea 5

## 13 Abstract

14 A modification in an existing water uptake and solute transport numerical model was implemented in  
15 order to allow the model to simulate solute uptake by the roots. The convection-dispersion equation  
16 (CDE) was solved numerically, using a complete implicit scheme, considering a transient state for water  
17 and solute fluxes and a soil solute concentration dependent boundary for the uptake at the root surface,  
18 based on the Michaelis-Menten (MM) equation. Additionally, a linear approximation was developed  
19 for the MM equation such that the CDE has a linear and a non-linear solution. A radial geometry  
20 was assumed, considering a single root with its surface acting as the uptake boundary and the outer  
21 boundary being the half distance between neighboring roots, a function of root density. The proposed  
22 solute transport model includes active and passive solute uptake and predicts solute concentration as a  
23 function of time and distance from the root surface. It also estimates the relative transpiration of the  
24 plant, on its turn directly affecting water and solute uptake and related to water and osmotic stress status  
25 of the plant. Performed simulations show that the linear and non-linear solutions result in significantly  
26 different solute uptake predictions when the soil solute concentration is below a limiting value ( $C_{lim}$ ). This  
27 reduction in uptake at low concentrations may result in a further reduction in the relative transpiration.  
28 The contributions of active and passive uptake vary with parameters related to the ion species, the plant,  
29 the atmosphere and the soil hydraulic properties. The model showed a good agreement with an analytical  
30 model that uses a linear concentration dependent equation as boundary condition for uptake at the root  
31 surface. The advantage of the numerical model is it allows simulation of transient solute and water  
32 uptake and, therefore, can be used in a wider range of situations. Simulation with different scenarios  
33 and comparison with experimental results are needed to verify model performance and possibly suggest  
34 improvements.

## 35 Introduction

36 Plant transpiration is directly affected by responses from abiotic stress like those related to excess or  
37 scarcity of water and solute in soil. Modeling arises as a relevant manner of predicting actual transpiration  
38 rates based on water and solute movement physical processes, improving predictions of crop growth and  
39 productivity. Models of water and solute uptakes are often classified as microscopic, which describe  
40 radial flow to single cylindrical roots (Gardner, 1965; Barber, 1974; Cushman, 1979; De Willigen and Van  
41 Noordwijk, 1994; Roose et al., 2001; De Jong van Lier et al., 2009), and macroscopic, which describe flow  
42 by adding a layered sink term added to the mass balance equations, without considering root geometry  
43 (Šimůnek et al., 2006; Somma et al., 1998; Van Dam et al., 2008). Microscopic models have the advantage  
44 to implicit simulate water uptake compensation as the uptake is controlled by computed local water  
45 potential gradients, whereas macroscopic can simulate processes at greater (plot or field) scales. As of  
46 water uptake models, water stress equations also enter in this classification. Macroscopic models for  
47 water stress (Feddes et al., 1978; Homaei, 1999; Li et al., 2006) are widely used but they fail when  
48 have the disadvantage of being overall empirical, with parameters that does not have a clear physical  
49 meaning. Microscopic models better cope with the phenomena as their physical underlying processes are  
50 translated in mathematical formulations. De Jong van Lier et al. (2006) proposed a microscopic root  
51 water uptake model that predicts the onset of the falling transpiration rate phase, according to a pressure  
52 head threshold value ( $h_{lim}$ ) which is determined by the potential matric flux ( $M$ ), function of potential  
53 transpiration and root length density. (SHOW EQUATION?) cite quirijn 2006 and everton 2016 Their  
54 approach brought a physical meaning and reduced the number of parameters of the uptake reduction  
55 function. In a later work, De Jong van Lier et al. (2009) introduced the osmotic component to generate  
56 a combined water and osmotic stress model.

Solute mobility in soil is described by the processes of convective transport by water mass flow and movement driven by diffusion due to the concentration gradient caused by solute depletion (or accumulation) in the root surface (Barber, 1962). The earlier analytical solutions for the convection-dispersion equation were formulated considering a steady state condition to the water flow and a solute uptake governed by the solute concentration in the soil solution (Barber, 1974; Cushman, 1979; Nye and Marriott, 1969) or determined by a constant plant demand (De Willigen, 1981). A solution considering a ‘pseudo-steady state’ for water flow and a solute concentration dependent uptake was later proposed by Roose et al. (2001). The concentration limiting (or supply driven) approach may overestimate the uptake in scenarios where solute supply to the root is not limiting (Barracough and Leigh, 1984) whilst the constant plant demand (or demand driven) formulation may overestimate the uptake when the soil is very dry or at low solute concentration at the root surface, when the diffusive flow prevails. The more realistic model considers both the supply driven uptake when solute in soil is limiting and the demand driven uptake when solute in soil is abundant. As the model gains complexity analytical solutions becomes unfeasible. Numerical models then plays a important role to compute solutions for complex nonlinear models of water and solute uptake, and can be used to estimate water and solute movement under transient conditions (CITE MODELS).

A nonlinear solute uptake boundary condition that can be used as a boundary condition at root surface and with a concentration dependent solute uptake is the Michaelis-Menten equation (Barber, 1995; Barber and Cushman, 1981; Schröder et al., 2012; Šimunek and Hopmans, 2009). The MM equation is supposed to describe well the solute uptake for both anions (Epstein, 1972; Siddiqi et al., 1990; Wang et al., 1993) and cations (Broadley et al., 2007; Kelly and Barber, 1991; Kochian and Lucas, 1982; Lux et al., 2011; Sadana et al., 2005) in the low concentration range and, adding a linear component to the equation, it can properly estimates the uptake rate also for higher concentrations (Borstlap, 1983; Broadley et al., 2007; Epstein, 1972; Kochian and Lucas, 1982; Vallejo et al., 2005; Wang et al., 1993). Many authors agree that for low concentration in external medium, the uptake is driven by an active plant mechanism, as it occurs contrary the solute gradient between root and soil (Epstein’s mechanism I). For the high concentration range, solutes are freely transported from soil to roots by diffusion and occasional convection. This passive transport is known as Epstein’s mechanism II (Kochian and Lucas, 1982; Siddiqi et al., 1990). Details on Epstein’s mechanisms and its physiological mechanisms, as well as on active and passive uptake, are found in Epstein (1960) and Fried and Shapiro (1961).

The values of MM parameters are strongly dependent on the experimental methods used and vary with plant species, plant age, plant nutritional status, soil temperature and pH (Barber, 1995; Shi et al., 2013). Therefore, they have to be determined for each particular experimental scenario. Some types of experiments to determine the kinetic parameters  $I_m$ ,  $K_m$  and  $C_{min}$  include hydroponically-grown plants (Barber, 1995) and the use of radioisotopes to estimate them directly from soil (Nye and Tinker, 1977). The latter is more realistic since there is a large difference between a stirred nutrient solution and the complex and dynamic soil medium. Measuring  $C_{min}$  is particularly difficult (Lambers et al., 2008; Seeling and Claassen, 1990) because it occurs at very low concentration levels that may be hard to be accurately measured. Seeling and Claassen (1990) show that  $C_{min}$  can be neglected for the cases of high  $K_m$  values.

The objective of this thesis is to present a modification of the model of root water uptake and solute transport proposed by De Jong van Lier et al. (2009). This modification allows the model to take into account plant solute uptake. To do so, a numerical mechanistic solution for the equation of convection-dispersion will be developed that considers transient flow of water and solute, as well as root competition. A soil concentration dependent solute uptake function as boundary condition at the root surface was assumed. In this way, the new model allows prediction of active and passive contributions to the solute uptake, which can be used to separate ionic and osmotic stresses by considering solute concentration inside the plant. The proposed model is compared with the original model, with a constant solute uptake numerical model and with an analytical model that uses a steady state condition for water content.

The model here proposed considers a supply driven solute uptake and gives opportunity to add a demand driven uptake when considering solute concentration inside the plant when needed.

## MATERIAL AND METHODS

### Soils and Hydraulic Properties

Water uptake was analyzed using hydraulic data for three topsoils from the Dutch Staring series (Wösten et al., 2001) as listed in Table 1. The Van Genuchten (1980) equation system was used to describe  $K-\theta-h$  relations for these soils:

$$\theta(h) = \theta_r + \frac{\theta_s - \theta_r}{[1 + |\alpha h|^n]^{1-(1/n)}} \quad (1)$$

$$K(\theta) = K_s \Theta^\lambda [1 - (1 - \Theta^{n/(n-1)})^{(1-(1/n))}]^2 \quad (2)$$

where  $\theta$  ( $\text{m}^3 \text{ m}^{-3}$ ) is the water content,  $K$  ( $\text{m s}^{-1}$ ) and  $K_s$  ( $\text{m s}^{-1}$ ) are respectively the hydraulic conductivity and the saturated hydraulic conductivity,  $h$  is the pressure head (m),  $\Theta$  (-) is the effective saturation defined by  $\frac{(\theta - \theta_r)}{(\theta_s - \theta_r)}$ ;  $\theta_s$  ( $\text{m}^3 \text{ m}^{-3}$ ) and  $\theta_r$  ( $\text{m}^3 \text{ m}^{-3}$ ) are the saturated and residual water contents, respectively; and  $\alpha$  ( $\text{m}^{-1}$ ),  $\lambda$  (-) and  $n$  (-) are empirical parameters.

Table 1: Soil hydraulic parameters used in simulations

Starting soil ID	Textural class	Reference in this paper	$\theta_r$ $\text{m}^3 \text{ m}^{-3}$	$\theta_s$ $\text{m}^3 \text{ m}^{-3}$	$\alpha$ $\text{m}^{-1}$	$\lambda$ -	$n$ -	$K_s$ $\text{m d}^{-1}$
B3	Loamy sand	Sand	0.02	0.46	1.44	-0.215	1.534	0.1542
B11	Heavy clay	Clay	0.01	0.59	1.95	-5.901	1.109	0.0453
B13	Sandy loam	Loam	0.01	0.42	0.84	-1.497	1.441	0.1298

## Model Description

Microscopic root uptake models consider a single cylindrical root of radius  $r_0$  (m) with an extraction zone being represented by a concentric cylinder of radius  $r_m$  (m) that bounds the half-distance between roots. The height of both cylinders is  $z$  (m) and represents the rooted soil depth. The basic assumptions of this type of model is that the root density does not change with depth and there is no difference in intensity of extraction along the root surface. Water and solute flows are axis-symmetric.

It is common to report root length density  $R$  ( $\text{m m}^{-3}$ ) and  $r_0$ . These are related to  $r_m$  and root length  $L$  (m) by the following equations:

$$r_m = \frac{1}{\sqrt{\pi R}} \quad (3)$$

$$L = \frac{A_p z}{\pi r_m^2} \quad (4)$$

where  $A_p$  ( $\text{m}^2$ ) is the soil surface area occupied by the plant.  $R$  also can be calculated from the assumed radial geometry by

$$R = \frac{1}{\pi r_m^2} . \quad (5)$$

The geometry of the soil-root system considers an uniformly distributed parallel cylindrical root of radius  $r_0$  and length  $z$ . To each root, a concentric cylinder of radius  $r_m$  and length  $z$  can be assigned to represent its extraction volume (Figure 1).

The discretization needed for the numerical solution was performed at the single root scale. As the extraction properties of the root are considered uniform along its length, and assuming no vertical differences in root density and fluxes, the cylinder can be represented by its cross-section: a circle. The area of this circle, representing the extraction region, was subdivided into  $n$  circular segments of variable size  $\Delta r$  (m), small near the root and increasing with distance, according to the equation De Jong van Lier et al. (2009):

$$\Delta r = \Delta r_{min} + (\Delta r_{max} - \Delta r_{min}) \left( \frac{r - r_0}{r_m - r_0} \right)^S \quad (6)$$

where the subscripts in  $\Delta r$  indicate the minimum and maximum segment sizes and  $S$  gives the rate at which the segment size increases. This variable size discretization has the advantage to result in smaller segments in regions that need more detail in the calculations (near the root soil interface) due to the greater variation of expected fluxes. Figure 2 shows a schematic representation of the discretization as projected by Equation 6.

The Richards equation for one-dimensional axis-symmetric flow can be written as

$$\frac{\partial \theta}{\partial t} = \frac{\partial \theta}{\partial H} \frac{\partial H}{\partial t} = C_w(H) \frac{\partial H}{\partial t} = \frac{1}{r} \frac{\partial}{\partial r} \left( r K(h) \frac{\partial H}{\partial r} \right) \quad (7)$$

where the total hydraulic head ( $H$ ) is the sum of pressure ( $h$ ) and osmotic ( $h_\pi$ ) heads and  $C_w$  ( $\text{m}^{-1}$ ) is the differential water capacity  $\frac{\partial \theta}{\partial H}$ . Analogous to Van Dam and Feddes (2000), Equation 7 can be solved using an implicit scheme of finite differences with the Picard iterative process:

$$C_{w_i}^{j+1,p-1} (H_i^{j+1,p} - H_i^{j+1,p-1}) + \theta_i^{j+1,p-1} - \theta_i^j = \frac{t^{j+1} - t^j}{r_i \Delta r_i} \times \left[ r_{i-1/2} K_{i-1/2}^j \frac{H_{i-1}^{j+1,p} - H_i^{j+1,p}}{r_i - r_{i-1}} - r_{i+1/2} K_{i+1/2}^j \frac{H_i^{j+1,p} - H_{i+1}^{j+1,p}}{r_{i+1} - r_i} \right] \quad (8)$$

where  $i$  ( $1 \leq i \leq n$ ) refers to the segment number,  $j$  is the time step and  $p$  the iteration level. The Picard's method is used to reduce inaccuracies in the implicit numerical solution for the  $h$ -based Equation 7 (Celia et al., 1990).

The solution for Equation 8 results in prediction of pressure head in soil as a function of time and distance from the root surface. The considered boundary conditions relate the flux density entering the root to the transpiration rate for the inner segment; and considers zero flux for the outer segment:

$$K(h) \frac{\partial h}{\partial r} = q = 0, \quad r = r_m \quad (9)$$

$$K(h) \frac{\partial h}{\partial r} = q_0 = \frac{T_p}{2\pi r_0 R z}, \quad r = r_0 \quad (10)$$

The computer algorithm that solves the Equation 8 and applies boundary conditions 9 and 10 can be found in Appendix ??.

The convection-dispersion equation for one-dimensional axis-symmetric flow can be written as

$$r \frac{\partial(\theta C)}{\partial t} = - \frac{\partial}{\partial r} (r q C) + \frac{\partial}{\partial r} \left( r D \frac{\partial C}{\partial r} \right). \quad (11)$$

with initial condition corresponding to constant solute concentration ( $C_{ini}$ ) in all segments:

$$C = C_{ini}, \quad t = 0, \quad r = r_i, \quad 1 \leq i \leq n. \quad (12)$$

Both boundary conditions are of the flux type, according to

$$-D(\theta) \frac{\partial C}{\partial r} \Big|_{r=r_i} + qC = F, \quad t > 0, \quad r_i = \{r_0, r_m\}. \quad (13)$$

From the assumed geometry (Figure 2) it follows that the boundary condition at the outer segment corresponds to zero solute flux ( $q_s$ ):

$$F = 0, \quad r = r_m. \quad (14)$$

The rate of solute uptake by plant roots can be described by the MM equation. Therefore, the uptake shape function  $\mu(C)$  can be supposed to follow the concentration dependent MM kinetics:

$$F = \mu(C) = \frac{C}{K_m + C} I_m \quad (15)$$

where  $I_m$  is the maximum uptake rate,  $C$  is the solute concentration in soil solution and  $K_m$  the Michaelis-Menten constant.  $I_m$  can be found experimentally and  $K_m$  is to be calibrated as the concentration at which  $I_m$  assumes half of its value, being interpreted as the affinity of the plant for the solute.

The boundary condition for solute transport at the root surface ( $r_0$ ) represents the concentration dependent solute uptake, described by the MM equation 15, with the following assumptions:

1. Solute uptake by mass flow of water is only controlled by the transpiration flow, a convective flow that is considered to be passive;
2. Plant regulated active uptake corresponds to diffusion;

- 183 3. Plant demand is equal to the  $I_m$  parameter from the MM equation;  
 184 4. At a soil solution concentration value  $C_{lim}$ , the solute flux limits the uptake.

185 We assume that the plant demand for solute is constant in time. The uptake, however, can be  
 186 higher or lower than the demand, depending on the concentration in the soil solution at the root surface  
 187 (Figure 3). If the concentration is bellow a certain limiting value ( $C_{lim}$ ), the uptake is limited by the  
 188 solute flux, *i.e.* solute flux can not attend plant demand even with potential values of active uptake.  
 189 Additionally, solute uptake by mass flow of water can be higher than the plant demand in situations of  
 190 high transpiration rate and/or for high soil water content. In these cases, we assume that active uptake  
 191 is zero and all uptake occurs by the passive process. A concentration  $C_2$  for this situation is calculated.  
 192 When the concentration is between  $C_{lim}$  and  $C_2$ , the uptake is equal to the plant demand as a result  
 193 of the sum of active and passive contributions to the uptake. Assumption 1 states that passive uptake  
 194 is not controlled by any physiological plant mechanisms and, in order to optimize the use of metabolic  
 195 energy, active uptake is regulated in such way that it works as a complementary mechanism of extraction  
 196 to achieve plant demand (Assumption 2). This results in a lower active uptake contribution than that  
 197 of its potential value. However, the effect of the solute concentration inside the plant on solute uptake  
 198 and plant demand is not considered in the model. Consequently, a scenario for which the demand is  
 199 reduced due to an excess of solute concentration in the plant is also not considered. This might lead to  
 200 an overestimated prediction of uptake.

201 A piecewise non-linear uptake function that considers these explicit boundary conditions was formu-  
 202 lated as:

$$203 \quad F = \begin{cases} \frac{I_m C_0}{K_m + C_0} + q_0 C_0, & \text{if } C_0 < C_{lim} \\ I_m, & \text{if } C_{lim} \leq C_0 \leq C_2 \\ q_0 C_0, & \text{if } C_0 > C_2 \end{cases} \quad (16)$$

$$(17)$$

$$(18)$$

204 with  $C_{lim}$  determined by the positive root of

$$205 \quad C_{lim} = -\frac{K_m \pm (K_m^2 + 4I_m K_m / q_0)^{1/2}}{2}, \quad (19)$$

206 and  $C_2$  by

$$207 \quad C_2 = \frac{I_m}{q_0}. \quad (20)$$

208 The non-linear part of the uptake function resides in Equation 16. As implicit numerical implemen-  
 209 tations of non-linear functions may result in solutions with stability issues, a linearization of Equation 16  
 210 was made, resulting in:

$$211 \quad F = (\alpha + q_0) C_0, \quad \text{if } C_0 < C_{lim} \quad (21)$$

212 where  $\alpha$  ( $\text{m s}^{-1}$ ) and  $q_0$  ( $\text{m s}^{-1}$ ) are the active and passive contributions for the solute uptake slope  
 213 ( $\alpha + q_0$ ). This linearization is very similar to the one proposed by Tinker and Nye (2000), but does  
 214 not consider the solute concentration inside the plant. The derivation of Equations 19 to 21 is shown in  
 215 Appendix ??.

216 Finally, the boundary condition at the inner segment refers to the concentration dependent solute  
 217 flux at the root surface ( $F$ ,  $\text{mol m}^{-2} \text{d}^{-1}$ ) in agreement to Equation and 21 for the non-linear and linear  
 218 case, respectively. The uptake of each root equals  $-F/R$  ( $\text{mol d}^{-1}$ , the negative sign indicating solute  
 219 depletion), thus, the condition at the root surface is described by:

$$220 \quad -D(\theta) \frac{\partial C}{\partial r} + q_0 C_0 = q_{s_0} = -\frac{F}{2\pi r_0 R z}, \quad r = r_0. \quad (22)$$

## 221 Numerical implementation

222 TELL THAT THERE IS ALSO A LINEAR SOLUTION BUT IT WONT BE SHOWN IN THE PAPER.  
 223 ALSO, THAT IT WONT BE SHOWN THE SOLUTIONS FOR THE COMPARED MODELS. CITE  
 224 THE THESIS.

225 A fully implicit numerical treatment was given to the water and solute balance equations 7 and 11.  
 226 In the numerical solution, the combined water and solute movement is simulated iteratively. In a first

step, the water movement towards the root is simulated, assuming salt concentrations from the previous time step. In a second step, the salt contents per segment are updated and new values for the osmotic head in all segments are calculated. The first step is then repeated with updated values for the osmotic heads. This process is repeated until the pressure head values and osmotic head values between iterations converge.

The implicit numerical discretization of Equation 11 yields:

$$\begin{aligned} \theta_i^{j+1} C_i^{j+1} - \theta_i^j C_i^j = & \frac{\Delta t}{2r_i \Delta r_i} \times \\ & \left\{ \frac{r_{i-1/2}}{r_i - r_{i-1}} \left[ q_{i-1/2} (C_{i-1}^{j+1} \Delta r_i + C_i^{j+1} \Delta r_{i-1}) - 2D_{i-1/2}^{j+1} (C_i^{j+1} - C_{i-1}^{j+1}) \right] - \right. \\ & \left. \frac{r_{i+1/2}}{r_{i+1} - r_i} \left[ q_{i+1/2} (C_i^{j+1} \Delta r_{i+1} + C_{i+1}^{j+1} \Delta r_i) - 2D_{i+1/2}^{j+1} (C_{i+1}^{j+1} - C_i^{j+1}) \right] \right\} \end{aligned} \quad (23)$$

Applying equation 23 to each segment, the concentrations for the next time step  $C_i^{j+1}$  (mol m<sup>-3</sup>) are obtained by solving the following tridiagonal matrix:

$$\begin{bmatrix} b_1 & c_1 & & & & \\ a_2 & b_2 & c_2 & & & \\ & a_3 & b_3 & c_3 & & \\ & & \ddots & \ddots & \ddots & \\ & & & a_{n-1} & b_{n-1} & c_{n-1} \\ & & & & a_n & b_n \end{bmatrix} \begin{bmatrix} C_1^{j+1} \\ C_2^{j+1} \\ C_3^{j+1} \\ \vdots \\ C_{n-1}^{j+1} \\ C_n^{j+1} \end{bmatrix} = \begin{bmatrix} f_1 \\ f_2 \\ f_3 \\ \vdots \\ f_{n-1} \\ f_n \end{bmatrix} \quad (24)$$

with  $f_i$  (mol m<sup>-2</sup>) defined as

$$f_i = r_i \theta_i^j C_i^j \quad (25)$$

and  $a_i$  (m),  $b_i$  (m) and  $c_i$  (m) defined for the respective segments as described in the following.

1. The intermediate nodes ( $i = 2$  to  $i = n - 1$ )

Rearrangement of Equation 23 to 24 results in the coefficients:

$$a_i = - \frac{r_{i-1/2} (2D_{i-1/2}^{j+1} + q_{i-1/2} \Delta r_i) \Delta t}{2(r_i - r_{i-1}) \Delta r_i} \quad (26)$$

$$b_i = r_i \theta_i^{j+1} + \frac{\Delta t}{2\Delta r_i} \left[ \frac{r_{i-1/2}}{(r_i - r_{i-1})} (2D_{i-1/2}^{j+1} - q_{i-1/2} \Delta r_{i-1}) + \frac{r_{i+1/2}}{(r_{i+1} - r_i)} (2D_{i+1/2}^{j+1} + q_{i+1/2} \Delta r_{i+1}) \right] \quad (27)$$

$$c_i = - \frac{r_{i+1/2} \Delta t}{2\Delta r_i (r_{i+1} - r_i)} (2D_{i+1/2}^{j+1} - q_{i+1/2} \Delta r_i) \quad (28)$$

2. The outer boundary ( $i = n$ )

Applying boundary condition of zero solute flux, the third and fourth terms from the right hand side of Equation 23 are equal to zero. Thus, the solute balance for this segment is written as:

$$\begin{aligned} \theta_n^{j+1} C_n^{j+1} - \theta_n^j C_n^j = & \frac{\Delta t}{2r_n \Delta r_n} \times \\ & \left\{ \frac{r_{n-1/2}}{r_n - r_{n-1}} \left[ q_{n-1/2} (C_{n-1}^{j+1} \Delta r_n + C_n^{j+1} \Delta r_{n-1}) - \right. \right. \\ & \left. \left. 2D_{n-1/2}^{j+1} (C_n^{j+1} - C_{n-1}^{j+1}) \right] \right\} \end{aligned} \quad (29)$$

Rearrangement of Equation 29 to 24 results in the coefficients:

$$a_n = -\frac{r_{n-1/2}(2D_{n-1/2}^{j+1} + q_{n-1/2}\Delta r_n)\Delta t}{2(r_n - r_{n-1})\Delta r_n} \quad (30)$$

$$b_n = r_n\theta_n^{j+1} + \frac{\Delta t}{2\Delta r_n} \left[ \frac{r_{n-1/2}}{r_n - r_{n-1}} (2D_{n-1/2}^{j+1} + q_{n-1/2}\Delta r_{n-1}) \right] \quad (31)$$

245 3. The inner boundary ( $i = 1$ )

246 (a) For  $C < C_{lim}$

247 Applying boundary conditions of non-linear concentration dependent solute flux, the first and  
 248 second term of the right-hand side of Equation 23 become  $-\left(\frac{I_m}{2\pi r_0 R_z(K_m + C_1^{j+1})} + q_0\right)C_1^{j+1}\Delta r_1$ :

$$\theta_1^{j+1}C_1^{j+1} - \theta_1^jC_1^j = \frac{\Delta t}{2r_1\Delta r_1} \times \left\{ \begin{aligned} &\frac{r_{1-1/2}}{r_1 - r_0} \left[ -\left(\frac{I_m}{2\pi r_0 R_z(K_m + C_1^{j+1})} + q_0\right) C_1^{j+1}\Delta r_1 - \right. \\ &\left. \frac{r_{1+1/2}}{r_2 - r_1} \left[ \frac{q_{1+1/2}(C_1^{j+1}\Delta r_2 + C_2^{j+1}\Delta r_1) -}{2D_{1+1/2}^{j+1}(C_2^{j+1} - C_1^{j+1})} \right] \right] \end{aligned} \right\} \quad (32)$$

249 Rearrangement of Equation 32 to 24 results in the following coefficients:

$$b_1 = r_1\theta_1^{j+1} + \frac{\Delta t}{2\Delta r_1} \left[ \frac{r_{1+1/2}}{(r_2 - r_1)} (2D_{1+1/2}^{j+1} + q_{1+1/2}\Delta r_2) + \frac{r_{1-1/2}}{r_1 - r_0} \left( \frac{I_m}{2\pi r_0 R_z(K_m + C_1^{j+1})} + q_0 \right) \Delta r_1 \right] \quad (33)$$

$$c_1 = -\frac{r_{1+1/2}\Delta t}{2\Delta r_1(r_2 - r_1)} (2D_{1+1/2}^{j+1} - q_{1+1/2}\Delta r_1) \quad (34)$$

250 (b) For  $C_{lim} < C < C_2$

251 The constant uptake solution is based on the model proposed by De Willigen and Van No-  
 252 ordwijk (1994). The boundary condition at the root surface (Equation 22) corresponds to  
 253 constant solute flux, considering  $F = I_m$ :

$$q_{s0} = -\frac{I_m}{2\pi r_0 R_z}. \quad (35)$$

255 Applying boundary conditions of constant solute flux (Equation 35), the first and second term  
 256 of the right-hand side of Equation 23 become  $-\frac{I_m}{2\pi r_0 R_z}\Delta r_1$  for  $C > 0$ :

$$\theta_1^{j+1}C_1^{j+1} - \theta_1^jC_1^j = \frac{\Delta t}{2r_1\Delta r_1} \times \left\{ \begin{aligned} &\frac{r_{1-1/2}}{r_1 - r_0} \left( -\frac{I_m}{2\pi r_0 R_z} \right) \Delta r_1 - \\ &\frac{r_{1+1/2}}{r_2 - r_1} \left[ \frac{q_{1+1/2}(C_1^{j+1}\Delta r_2 + C_2^{j+1}\Delta r_1) -}{2D_{1+1/2}^{j+1}(C_2^{j+1} - C_1^{j+1})} \right] \end{aligned} \right\} \quad (36)$$

257 Introduction of Equation 36 in the tridiagonal matrix 24 results in the following coefficients:

$$b_1 = r_1\theta_1^{j+1} + \frac{\Delta t}{2\Delta r_1} \left[ \frac{r_{1+1/2}}{(r_2 - r_1)} (2D_{1+1/2}^{j+1} + q_{1+1/2}\Delta r_2) \right] \quad (37)$$

$$c_1 = -\frac{r_{1+1/2}\Delta t}{2\Delta r_1(r_2 - r_1)} (2D_{1+1/2}^{j+1} - q_{1+1/2}\Delta r_1) \quad (38)$$



258 and the  $f$  coefficient changes to:

$$f_1 = r_1 \theta_1^j C_1^j - \frac{r_{1+1/2}}{r_1 - r_0} I_m \frac{\Delta t}{4\pi r_0 R z} \quad (39)$$

259 (c) For  $\mathbf{C} = \mathbf{0}$

260 The zero uptake solution is based on the model proposed by De Jong van Lier et al. (2009).  
 261 The boundary condition at the root surface (Equation 22) corresponds to constant solute flux,  
 262 considering  $F = 0$ :

$$263 \quad q_{s0} = 0 \quad (40)$$

264 Applying boundary condition of zero solute flux, the first and second term of the right-hand  
 265 side of Equation 23 are equal to zero:

$$\begin{aligned} \theta_1^{j+1} C_1^{j+1} - \theta_1^j C_1^j &= \frac{\Delta t}{2r_1 \Delta r_1} \times \\ &\left\{ \frac{r_{1+1/2}}{r_2 - r_1} \left[ -q_{1+1/2} (C_1^{j+1} \Delta r_2 + C_2^{j+1} \Delta r_1) + \right. \right. \\ &\quad \left. \left. 2D_{1+1/2}^{j+1} (C_2^{j+1} - C_1^{j+1}) \right] \right\} \end{aligned} \quad (41)$$

266 Introduction of Equation 41 in the tridiagonal matrix 24 results in the following coefficients:

$$b_1 = r_1 \theta_1^{j+1} + \frac{\Delta t}{2\Delta r_1} \left[ \frac{r_{1+1/2}}{(r_2 - r_1)} (2D_{1+1/2}^{j+1} + q_{1+1/2} \Delta r_2) \right] \quad (42)$$

$$c_1 = -\frac{r_{1+1/2} \Delta t}{2\Delta r_1 (r_2 - r_1)} (2D_{1+1/2}^{j+1} - q_{1+1/2} \Delta r_1) \quad (43)$$

## 267 Simulation Scenarios

268 The simulations were performed using the hydraulic parameters from the Dutch Staring series Wösten  
 269 et al. (2001) for three different soils types, as listed in Table 1. The general system parameters for the  
 270 different scenarios are listed in Table 2 and values for the Michaelis-Menten (MM) parameters in Table 3.  
 271 Values of root length density, initial solute concentration, relative transpiration, soil type, and ion species  
 272 were chosen at several values, composing eight distinct scenarios as listed in Table 4. Scenario 1 was  
 273 considered as default, the other scenarios derive from scenario 1 by changing only one input parameter.  
 274 In this way, the effect of variation in soil hydraulic properties is exemplified by scenarios 1, 6 and 7; root  
 275 length density by scenarios 1, 4 and 5; initial solute concentration by scenarios 1 and 3; and potential  
 276 transpiration by scenarios 1 and 2.

277 The default values of  $\Delta r_{min}$ ,  $\Delta r_{max}$  and  $S$  in Equation 6 were  $10^{-5}$  m,  $5 \cdot 10^{-4}$  m and 0.5, resulting  
 278 in 22, 68 and 213 segments for the high, medium and low root density simulations, respectively. To  
 279 guarantee complete convergence for the non-linear model, a time step of 0.01 s was used when  $C_0 < C_{lim}$ .  
 280 Parameters  $h_{ini}$  and  $C_{ini}$  were chosen such that the plant is in a no stress condition ( $T_r = 1$ ). All  
 281 simulation scenarios ended when  $T_r \leq 0.001$ , at that point considering water uptake to be negligible.

## 282 Analysis of linear and non-linear approaches

283 Relative and absolute differences, as well as the non-parametric Mann-Whitney U test, were calculated  
 284 to quantify how similar both solutions are.

285 NLU solution uses the non-linear MM equation and, due to an additional iterative process in the  
 286 numerical implementation, more time is needed to compute the results when compared with the linear  
 287 solution LU. It is also susceptible to numerical stability issues, depending on selected time and space  
 288 steps. On the other hand, LU is a simplified version of the MM equation in a way that the solute uptake  
 289 rate for  $C_0 < C_{lim}$  is always smaller than that of the original non-linear equation. It has no stability  
 290 problems and needs less computational time because it is less sensitive to space and time steps. In a first  
 291 analysis, the objective was to check if the difference in the results generated by the linearization of the  
 292 MM equation is sufficiently large to be properly analyzed. To do so, four different scenarios were chosen  
 293 (scenarios 1 to 4 as listed in Table 4).

Table 2: System parameters used in simulations scenarios

Description	Symbol	Scenario description	Value	Unit
Root radius	$r_0$		0.5	mm
Root depth	$z$		20	cm
Limiting root potential	$h_{lim}$		-150	m
Root density	$R$	Low root density	0.01	$\text{cm cm}^{-3}$
		Medium root density	0.1	
		High root densit	1	
Half distance between roots	$r_m$	Low root density	56.5	mm
		Medium root density	17.8	
		High root densit	5.65	
Potential transpiration rate	$T_p$	Low	3	$\text{mm d}^{-1}$
		High	6	
Initial solute concentration in bulk soil	$C_{ini}$	Low	1	$\text{mol m}^{-3}$
		High	10	
Initial pressure head	$h_{ini}$		-1	m
Diffusion coefficient in water	$D_{m,w}$		$1.98 \cdot 10^{-9}$	$\text{m}^2 \text{s}^{-1}$
Dispersivity	$\tau$		0.0005	m
Soil type		Sand	Table 1	
		Clay		
		Loam		

Table 3: Michaelis-Menten parameters for some solutes

Solute	$I_m$ $\text{mol m}^{-2} \text{s}^{-1}$	$K_m$ $\text{mol m}^{-3}$
$\text{NO}_3^-$	$10^{-5}$	0.05
$\text{K}^+$	$2 \cdot 10^{-6}$	0.025
$\text{H}_2\text{PO}_4^-$	$10^{-6}$	0.005
$\text{Cd}^{2+}$	$10^{-6}$	1

Table 4: Simulation scenarios

Scenario	$R$	$C_{ini}$	$T_p$	Soil	Ion
1	M	H	H	Loam	$\text{K}^+$
2	M	H	L	Loam	$\text{K}^+$
3	M	L	H	Loam	$\text{K}^+$
4	H	H	H	Loam	$\text{K}^+$
5	L	H	H	Loam	$\text{K}^+$
6	M	H	H	Sand	$\text{K}^+$
7	M	H	H	Clay	$\text{K}^+$
8	M	H	H	Loam	$\text{NO}_3^-$

## 294 Sensitivity analysis

295 The relative partial sensitivity  $\eta$  (de Jong van Lier et al., 2015) of model predictions  $Y$  as a function of  
296 the respective parameter value  $P$  was calculated as

$$297 \quad \eta = \frac{dY/Y}{dP/P} \quad (44)$$

298 where  $P$  is the default value of the parameter,  $dP$  is the in(de)crement applied to  $P$ ,  $Y$  is the output  
299 of a selected predicted variable and  $dY$  is the variation over  $Y$  when applied the new parameter value  
300  $P \pm dP$ .

301 To determine the sensitivity of the model to an input parameter, the magnitude of its derivative in  
302 respect of the model result is calculated. If this derivative is close to zero, the model has a low sensitivity  
303 to the respective parameter. The higher the derivative, the higher is the sensitivity and, therefore, the  
304 higher is the precision required when determining that parameter. By making a relative analysis like in  
305 Equation 44, the sensitivity for distinct parameters can be compared.

306 To determine the sensitivity, a  $dP/P$  of 0.01 (1%) was used for the following selected parameters: a)  
307 MM parameters  $I_m$ ,  $K_m$ ; and b) soil hydraulic parameters  $\alpha$ ,  $n$ ,  $\lambda$ ,  $K_s$ ,  $\theta_r$  and  $\theta_s$ . The analyzed predicted  
308 variables ( $Y$ ) were: time to completion of simulation  $t_{end}$ , osmotic head at completion of simulation  $h_\pi$ ,  
309 pressure head at completion of simulation  $h$ , average osmotic head in the soil profile at completion of  
310 simulation  $\bar{h}_\pi$ , average pressure head in soil profile at completion of simulation  $\bar{h}$  and accumulated uptake  
311 at completion of simulation  $Ac$ .

## 312 RESULTS AND DISCUSSION

313 Cite (Carillo et al., 2011) when talking about the first and second reductions in  $T_r$ . It is similar to the  
314 reductions in plant growth due to osmotic and ionic stresses.

## 315 Acknowledgements

316 The first author would like to thank to the National Counsel of Technological and Scientific Development  
317 (CNPq) for the scholarship granted during his PhD, to Coordination for the Improvement of Higher  
318 Education Personnel (CAPES) for the scholarship granted during the sandwich internship at Wageningen  
319 University, the Netherlands, and also to Peter de Willigen for his valuable contributions in the formulation  
320 of the mathematical framework of this study.

## 321 References

- 322 S A Barber. Influence of the plant root on ion movement in soil. In E W Carson, editor, *The plant root*  
323 *and its environment*, pages 525–564. Procedures in plant roots and their environment, Charlottesville,  
324 1974.
- 325 S A Barber and J H Cushman. Nitrogen uptake model for agronomic crops. In I K Iskander, editor,  
326 *Modelling wastewater renovation for land treatment*, pages 382–489. Wiley Interscience, New York,  
327 1981.
- 328 Stanley A Barber. A diffusion and mass-flow concept of soil nutrient availability. *Soil Science*, 93(1):  
329 39–49, 1962.
- 330 Stanley A Barber. *Soil nutrient bioavailability: a mechanistic approach*. John Wiley & Sons, New York,  
331 2 edition, 1995.
- 332 P B Barraclough and R A Leigh. The growth and activity of winter wheat roots in the field: the effect of  
333 sowing date and soil type on root growth of high-yielding crops. *The Journal of Agricultural Science*,  
334 103(01):59–74, 1984.
- 335 AC Borstlap. The use of model-fitting in the interpretation of dual uptake isotherms. *Plant, Cell &*  
336 *Environment*, 6(5):407–416, 1983.

- 337 Martin R Broadley, Philip J White, John P Hammond, Ivan Zelko, and Alexander Lux. Zinc in plants.  
338 *New Phytologist*, 173(4):677–702, 2007.
- 339 P Carillo, M G Annunziata, G Pontecorvo, A Fuggi, and P Woodrow. Salinity stress and salt tolerance.  
340 In Arun Shanker, editor, *Abiotic Stress in Plants – Mechanisms and Adaptations*, pages 21–38. inTech,  
341 Rijeka, 2011.
- 342 Michael A Celia, Efthimios T Bouloutas, and Rebecca L Zarba. A general mass-conservative numerical  
343 solution for the unsaturated flow equation. *Water resources research*, 26(7):1483–1496, 1990.
- 344 John H. Cushman. An analytical solution to solute transport near root surfaces for low initial concen-  
345 tration: I. equations development. *Soil Science Society of America Journal*, 43(6):1087–1090, 1979.
- 346 Quirijn De Jong van Lier, Klaas Metselaar, and Jos C. Van Dam. Root water extraction and limiting soil  
347 hydraulic conditions estimated by numerical simulation. *Vadose Zone Journal*, 5(4):1264–1277, 2006.
- 348 Quirijn De Jong van Lier, Jos C. Van Dam, and Klaas Metselaar. Root water extraction under combined  
349 water and osmotic stress. *Soil Science Society of America Journal*, 73(3):862–875, 2009.
- 350 Quirijn de Jong van Lier, Ole Wendroth, and Jos C. van Dam. Prediction of winter wheat yield with the  
351 swap model using pedotransfer functions: An evaluation of sensitivity, parameterization and prediction  
352 accuracy. *Agricultural Water Management*, 154(1):29–42, 2015.
- 353 Peter De Willigen. Mathematical analysis of diffusion and mass flow of solutes to a root assuming constant  
354 uptake. Technical report, Instituut voor Bodemvruchtbaarheid, Haren, 1981. Technical Report.
- 355 Peter De Willigen and Meine Van Noordwijk. Mass flow and diffusion of nutrients to a root with constant  
356 or zero-sink uptake i. constant uptake. *Soil science*, 157(3):162–170, 1994.
- 357 Emanuel Epstein. Spaces, barriers, and ion carriers: ion absorption by plants. *American Journal of*  
358 *Botany*, 47(5):393–399, 1960.
- 359 Emanuel Epstein. *Mineral nutrition of plants: principles and perspectives*. Science Reviews 2000, London,  
360 1972.
- 361 Reinder A Feddes, Piotr J Kowalik, and Henryk Zaradny. *Simulation of field water use and crop yield*.  
362 Centre for Agricultural Publishing and Documentation, Wageningen, 1978.
- 363 Maurice Fried and Raymond E Shapiro. Soil-plant relationships in ion uptake. *Annual Review of Plant*  
364 *Physiology*, 12(1):91–112, 1961.
- 365 W R Gardner. Dynamic aspects of soil-water availability to plants. *Annual review of plant physiology*,  
366 16(1):323–342, 1965.
- 367 Mehdi Homaei. *Root water uptake under non-uniform transient salinity and water stress*. PhD thesis,  
368 Wageningen University, 1999.
- 369 J M Kelly and S A Barber. Magnesium uptake kinetics in loblolly pine seedlings. *Plant and soil*, 134(2):  
370 227–232, 1991.
- 371 Leon V Kochian and William J Lucas. Potassium transport in corn roots i. resolution of kinetics into a  
372 saturable and linear component. *Plant Physiology*, 70(6):1723–1731, 1982.
- 373 Hans Lambers, F Stuart Chapin III, and Thijs L Pons. *Plant water relations*, chapter Chapter 3, pages  
374 163–223. Springer, New York, 2008.
- 375 K. Y. Li, R. De Jong, M. T. Coe, and N. Ramankutty. Root-water-uptake based upon a new water stress  
376 reduction and an asymptotic root distribution function. *Earth Interactions*, 10(14):1–22, 2006.
- 377 Alexander Lux, Michal Martinka, Marek Vaculík, and Philip J White. Root responses to cadmium in the  
378 rhizosphere: a review. *Journal of Experimental Botany*, 62(1):21–37, 2011.
- 379 P H Nye and F H C Marriott. A theoretical study of the distribution of substances around roots resulting  
380 from simultaneous diffusion and mass flow. *Plant and Soil*, 30(3):459–472, 1969.

- 381 Peter Hague Nye and Philip Bernard Tinker. *Solute movement in the soil-root system*. University of  
382 California Press, Berkeley, 1977.
- 383 Tiina Roose, A C Fowler, and P R Darrah. A mathematical model of plant nutrient uptake. *Journal of*  
384 *mathematical biology*, 42(4):347–360, 2001.
- 385 Upkar Singh Sadana, Parmodh Sharma, Nelson Castañeda Ortiz, Debasmita Samal, and Norbert  
386 Claassen. Manganese uptake and mn efficiency of wheat cultivars are related to mn-uptake kinet-  
387 ics and root growth. *Journal of Plant Nutrition and Soil Science*, 168(4):581–589, 2005.
- 388 Natalie Schröder, Mathieu Javaux, Jan Vanderborght, Bernhard Steffen, and Harry Vereecken. Effect of  
389 root water and solute uptake on apparent soil dispersivity: A simulation study. *Vadose Zone Journal*,  
390 11(3):1–14, 2012.
- 391 Björn Seeling and Norbert Claassen. A method for determining michaelis-menten kinetic parameters of  
392 nutrient uptake for plants growing in soil. *Zeitschrift für Pflanzenernährung und Bodenkunde*, 153(5):  
393 301–303, 1990.
- 394 Jianchu Shi, Alon Ben-Gal, Uri Yermiyahu, Lichun Wang, and Qiang Zuo. Characterizing root nitrogen  
395 uptake of wheat to simulate soil nitrogen dynamics. *Plant and soil*, 363(1-2):139–155, 2013.
- 396 M Yaeesh Siddiqi, Anthony DM Glass, Thomas J Ruth, and Thomas W Rufty. Studies of the uptake of  
397 nitrate in barley i. kinetics of  $^{13}\text{no}_3$ -influx. *Plant Physiology*, 93(4):1426–1432, 1990.
- 398 J Šimunek, M Šejna, and M Th Van Genuchten. The hydrus software package for simulating the two-and  
399 three-dimensional movement of water, heat, and multiple solutes in variably-saturated media. *Technical*  
400 *manual*, 1(1):241, 2006.
- 401 Jiří Šimunek and Jan W Hopmans. Modeling compensated root water and nutrient uptake. *Ecological*  
402 *modelling*, 220(4):505–521, 2009.
- 403 F Somma, J W Hopmans, and V Clausnitzer. Transient three-dimensional modeling of soil water and  
404 solute transport with simultaneous root growth, root water and nutrient uptake. *Plant and Soil*, 202  
405 (2):281–293, 1998.
- 406 P.B. Tinker and P.H. Nye. *Solute Movement in the Rhizosphere*. Topics in sustainable agronomy. Oxford  
407 University Press, 2000.
- 408 Augusto J Vallejo, Maria Luisa Peralta, and GUILLERMO E SANTA-MARIA. Expression of potassium-  
409 transporter coding genes, and kinetics of rubidium uptake, along a longitudinal root axis. *Plant, Cell*  
410 *& Environment*, 28(7):850–862, 2005.
- 411 Jos C Van Dam and Reinder A Feddes. Numerical simulation of infiltration, evaporation and shallow  
412 groundwater levels with the richards equation. *Journal of Hydrology*, 233(1):72–85, 2000.
- 413 Jos C Van Dam, Piet Groenendijk, Rob F A Hendriks, and Joop G Kroes. Advances of modeling water  
414 flow in variably saturated soils with swap. *Vadose Zone Journal*, 7(2):640–653, 2008.
- 415 M Th Van Genuchten. A closed-form equation for predicting the hydraulic conductivity of unsaturated  
416 soils. *Soil science society of America journal*, 44(5):892–898, 1980.
- 417 Miao Yuan Wang, M Yaeesh Siddiqi, Thomas J Ruth, and Anthony DM Glass. Ammonium uptake by  
418 rice roots (ii. kinetics of  $^{13}\text{nh}_4^+$  influx across the plasmalemma). *Plant physiology*, 103(4):1259–1267,  
419 1993.
- 420 J H M Wösten, G J Veerman, W J M De Groot, and J Stolte. Waterretentie-en doorlatendheidskarak-  
421 teristieken van boven-en ondergronden in nederland: de staringsreeks. 2001.

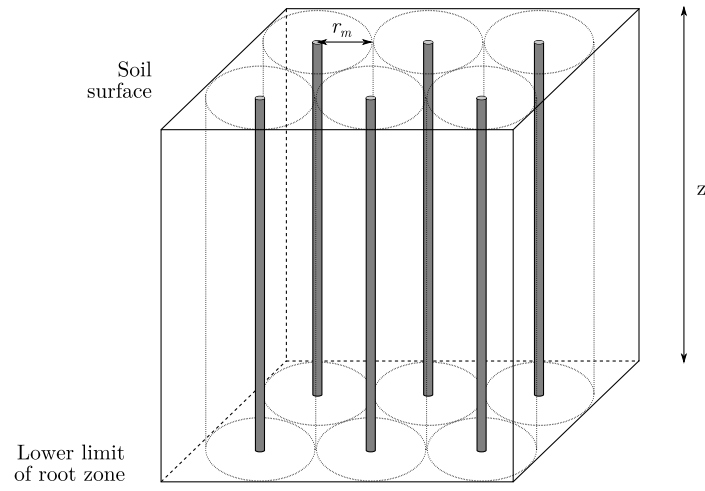


Figure 1: Schematic representation of the spatial distribution of roots in the root zone

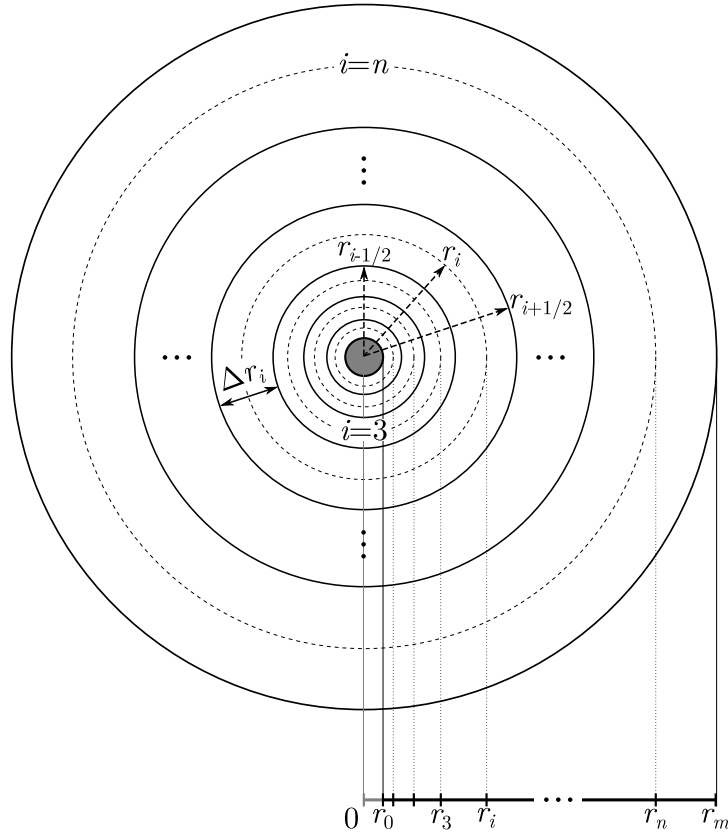


Figure 2: Schematic representation of the discretized domain considered in the model.  $\Delta r$  is the variable segment size, increasing with the distance from the root surface ( $r_0$ ) to the half-distance between roots ( $r_m$ ), and  $n$  is the number of segments

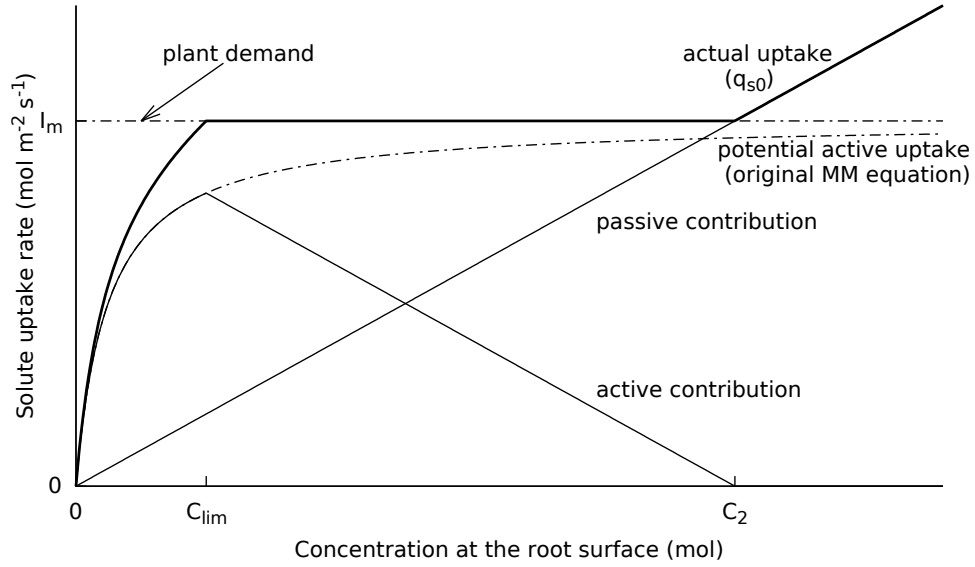


Figure 3: Solute uptake piecewise equation from MM equation 15 with boundary conditions. The bold line represents the actual uptake, thin lines represent active and passive contributions to the actual uptake, and dotted lines represent the plant demand and the potential active uptake